Structural Engineering and Mechanics, *Vol. 59, No. 6 (2016) 1095-1120*
DOI: http://dx.doi.org/10.12989/sem.2016.59.6.1095

Structural behavior of cable-stayed bridges after cable failure

Seungjun Kim[1a] and Young Jong Kang[*2]

[1]*Department of Construction Safety and Disaster Prevention Engineering, Daejeon University, 62 Daehak-ro, Dong-gu, Daejeon 34520, Republic of Korea*
[2]*School of Architectural, Civil and Environmental Engineering, Korea University, 145 Anam-ro, Seoul 02841, Republic of Korea*

(Received January 2, 2016, Revised May 21, 2016, Accepted May 27, 2016)

Abstract. This paper investigates the change of structural characteristics of steel cable-stayed bridges after cable failure. Cables, considered as the intermediate supports of cable-stayed bridges, can break or fail for several reasons, such as fire, direct vehicle clash accident, extreme weather conditions, and fatigue of cable or anchorage. Also, the replacement of cables can cause temporary disconnection. Because of the structural characteristics with various geometric nonlinearities of cable-stayed bridges, cable failure may cause significant change to the structural state and ultimate behavior. Until now, the characteristics of structural behavior after cable failure have rarely been studied. In this study, rational cable failure analysis is suggested to trace the new equilibrium with structural configuration after the cable failure. Also, the sequence of ultimate analysis for the structure that suffers cable failure is suggested, to study the change of ultimate behavior and load carrying capacity under specific live load conditions. Using these analysis methods, the statical behavior after individual cable failure is studied based on the change of structural configuration, and distribution of internal forces. Also, the change of the ultimate behavior and load carrying capacity under specific live load conditions is investigated, using the proposed analysis method. According to the study, significant change of the statical behavior and ultimate capacity occurs although just one cable fails.

Keywords: cable-stayed bridges; cable failure; cable failure analysis; nonlinear analysis; ultimate analysis

1. Introduction

Cable-stayed bridges are the most popular system for long-span bridges, because of their structural efficiency combined with good aesthetics. The bridge consists of girder, mast and stay cables. The flexural strength of the girder, compressive strength of the mast and tensile strength of stay cables are combined in the system, and the structural efficiency is maximized with rational design and construction methods. Among those main members, cables are designed as the intermediate support for the girder, instead of many columns or piers. So, cable-stayed bridges can be the most suitable system for long-span bridges, because of the intermediate support that the cables provide.

∗Corresponding author, Professor, E-mail: yjkang@korea.ac.kr
[a]Assistant Professor, E-mail: skim@dju.kr

Copyright © 2016 Techno-Press, Ltd.
http://www.techno-press.org/?journal=sem&subpage=8 ISSN: 1225-4568 (Print), 1598-6217 (Online)

It is well known that cable-stayed bridges show various geometric and material nonlinearities, and their nonlinearities mainly affect structural behavior, because of their structural characteristics (Adeli and Zhang 1994, Xi and Kuang 1999, Ren 1999, Freire *et al*. 2006). Among various geometric nonlinearities, the girder-mast-cable interaction is a very interesting characteristic of cable-stayed bridges. The girder and mast are connected with each other via stay cables. By means of the applied tensile force, tight cables connect the girder and mast. Because of the coupled connectivity, the local behavior of one main member induces the local behavior of other members, and finally leads to the global structural behavior. Thus, it can be supposed that cable failure may clearly affect the global structural behavior.

Cable failure may occur for several reasons, such as fire, direct vehicle clash accident, fatigue of cable or anchorage, and so on. Moreover, a cable may be temporarily disconnected, during replacement work of cables. Cable failure means the loss of support, because the cables of cable-stayed bridges are the intermediate support. Also, failure may lead to significant change of structural state and ultimate behavior, because of the geometric characteristics with various nonlinearities of the structure. So, investigation of the structural change after cable failure should be studied by means of a rational research method.

Until now, study of the static and dynamic behavior of cable-stayed bridges has been widely performed. For the development of design and construction, study of the initial shape analysis method and construction method has been performed (Wang *et al*. 1993, Wang and Yang 1993, Reddy *et al*. 1999, Chen *et al*. 2000, Kim and Lee 2001, Wang *et al*. 2004, Cheng and Xiao 2007). The structural stability or ultimate behavior of cable-stayed bridges has been studied with eigenvalue analysis or nonlinear analysis (Ren 1999, Song and Kim 2007, Kim 2009). But these studies focus on the structural behavior of common, healthy structures. In other words, study of the development of rational cable-failure analysis, or the investigation of structural behavior after cable failure, has rarely been performed. Raftoyiannis *et al*. (2014) studied the 2-dimensional dynamic responses of cable-stayed bridges after sudden failure of stays.

In this study, the structural characteristics after cable failure are dealt with. For this study, an algorithm of cable failure analysis to trace the new structural state after the cable failure is suggested, using the backward process analysis method. An ultimate analysis procedure is also suggested to analyze the ultimate behavior of the structure that suffered the cable failure. Using the proposed analysis method, the change of structural state after cable failure is studied based on the change of structural configuration, and distribution of the important internal forces. Moreover, the change of ultimate behavior and load carrying capacity under specific live load cases is studied in detail.

2. Theoretical background

In this chapter, theoretical background of the analysis is introduced. Because of various nonlinearities of cable-stayed bridges, analysis should be performed based on the theory of nonlinear finite element analysis. So, nonlinear elements to model the main members of the structure, and a method to consider the material nonlinearities, are introduced. Also, a numerical method for incremental-iterative analysis is described. After an introduction of the theoretical background of nonlinear analysis for cable-stayed bridges, an algorithm of cable failure analysis is described, which traces the statical structural state after cable failure. Finally, an ultimate analysis procedure for steel cable-stayed bridges after cable failure is suggested.

2.1 Finite elements, material nonlinearity consideration and incremental-iterative analysis strategy

2.1.1 Geometric and material nonlinearity consideration

It is well known that cable-stayed bridges show various geometric nonlinearities, such as the cable-sag effect, beam-column effect of the girder and mast, large-displacement effect and girder-mast-cable interaction. So, nonlinear finite elements should be used to model the main members, because of those various nonlinearities.

To model the girder and mast considered as beam-column members, a nonlinear frame element that has 2 nodes and 6 degrees of freedoms is used in this study. The element was derived based on the updated-Lagrangian formulation, and the local stiffness matrix of this element consists of elastic, geometric and induced matrices (Yang and Kuo 1994, Kim 2009). The following equation describes the stiffness matrix, composed of elastic, geometric and induced stiffness matrices.

$$[k] = [k_e] + [k_g] + [k_i] \tag{1}$$

where

$[k_e]$ = elastic stiffness matrix

$[k_g]$ = geometric stiffness matrix

$[k_i]$ = induced stiffness matrix

$$[k_g] = \begin{bmatrix} a & 0 & 0 & 0 & -d & -e & -a & 0 & 0 & 0 & -n & -o \\ & b & 0 & d & g & k & 0 & -b & 0 & n & -g & k \\ & & c & e & -h & g & 0 & 0 & -c & o & -h & -g \\ & & & f & i & l & 0 & -d & -e & -f & -i & -l \\ & & & & j & 0 & d & -g & h & -i & p & -q \\ & & & & & m & e & -k & -g & -l & q & r \\ & & & & & & a & 0 & 0 & 0 & n & o \\ & & & & & & & b & 0 & -n & g & -k \\ & & & & & & & & c & -o & h & g \\ & & & & & & & & & f & i & l \\ & & & & & & & & & & j & 0 \\ & & & & & & & & & & & m \end{bmatrix} \tag{2}$$

where

$$a = \frac{{}^1F_{xb}}{{}^1L},\quad b = \frac{6\,{}^1F_{xb}}{5\,{}^1L} + \frac{12\,{}^1F_{xb}I_z}{A\,{}^1L^3},\quad c = \frac{6\,{}^1F_{xb}}{{}^1L} + \frac{12\,{}^1F_{xb}I_y}{A\,{}^1L^3},\quad d = \frac{{}^1M_{ya}}{{}^1L},\quad e = \frac{{}^1M_{za}}{{}^1L}$$

$$f = \frac{{}^1F_{xb}J}{A\,{}^1L},\quad g = \frac{{}^1M_{xb}}{{}^1L},\quad h = \frac{{}^1F_{xb}}{10} + \frac{6\,{}^1F_{xb}I_y}{A\,{}^1L^2},\quad i = \frac{{}^1M_{za} + {}^1M_{zb}}{6},\quad j = \frac{2\,{}^1F_{xb}\,{}^1L}{15} + \frac{4\,{}^1F_{xb}I_y}{A\,{}^1L}$$

$$k = \frac{{}^1F_{xb}}{10} + \frac{6\,{}^1F_{xb}I_z}{A\,{}^1L^2},\quad l = -\frac{{}^1M_{ya} + {}^1M_{yb}}{6},\quad m = \frac{2\,{}^1F_{xb}\,{}^1L}{15} + \frac{4\,{}^1F_{xb}I_z}{A\,{}^1L},\quad n = \frac{{}^1M_{yb}}{{}^1L},\quad o = \frac{{}^1M_{zb}}{{}^1L}$$

$$p = \frac{{}^1F_{xb}\,{}^1L}{30} + \frac{2\,{}^1F_{xb}I_y}{A\,{}^1L},\quad q = -\frac{{}^1M_{xb}}{2},\quad r = -\frac{{}^1F_{xb}\,{}^1L}{30} + \frac{2\,{}^1F_{xb}I_z}{A\,{}^1L}$$

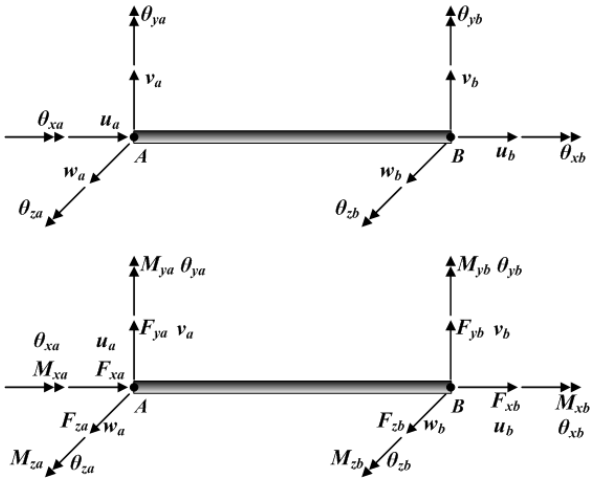

Fig. 1 Nodal displacements and forces of the nonlinear frame element

A = sectional area of the frame element
L = length of the frame element
I_y, I_z = 2nd moment of inertia with respect to the y and z axis, respectively
J = torsional constant

$$[k_i] = \begin{bmatrix} [0] & & & \\ & [k_i]_a & & \\ & & [0] & \\ & & & [k_i]_b \end{bmatrix} \tag{3}$$

where

$$[k_i]_a = \begin{bmatrix} 0 & 0 & 0 \\ {}^1M_{za} & 0 & -{}^1M_{xa}/2 \\ -{}^1M_{ya}/2 & {}^1M_{xa}/2 & 0 \end{bmatrix}$$

$$[k_i]_b = \begin{bmatrix} 0 & 0 & 0 \\ {}^1M_{zb} & 0 & -{}^1M_{xb}/2 \\ -{}^1M_{yb}/2 & {}^1M_{xb}/2 & 0 \end{bmatrix}$$

To model the cable member of cable-stayed bridges, a nonlinear equivalent truss element is used. This element was developed based on a nonlinear truss element, with an equivalent modulus derived to consider the sag effect of the stay cables. The stiffness matrix of the element consists of elastic stiffness and geometric stiffness, but the elastic modulus in the elastic stiffness is replaced by an equivalent modulus, which is derived based on the force-elongation relationship of the elastic catenary (Ernst 1965, Fleming 1979, Gimsing 1983). In general, the conventional equivalent modulus of a common equivalent truss element was derived with some simplification by Taylor's series. But in this study, an equivalent modulus derived without any simplification of

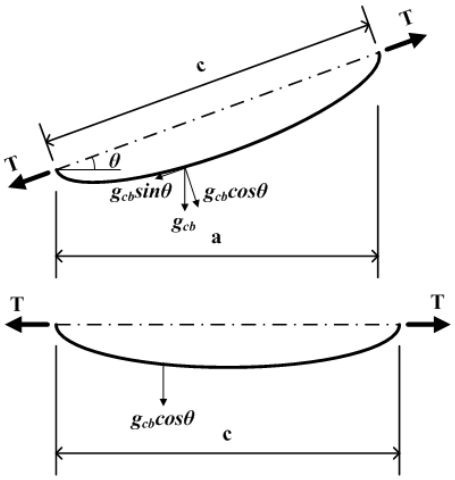

(g_{cb}: weight per unit length of a cable, T: tensile force)

Fig. 2 Inclined stay cable and equivalent horizontal stay cable with equal deformational characteristics

the force-elongation relationship of the elastic catenary was used (Song *et al*. 2006, Kim 2009). Eq. (4) shows the stiffness matrix of the nonlinear truss element while Eqs. (5) and (6) show the equivalent modulus for taking into account the nonlinear effect of the cable member considering the applied tensile force.

$$[k]=[k_e]+[k_g]=\frac{{}^1E_{eq}+{}^1A}{{}^1L}\begin{bmatrix}1&0&0&-1&0&0\\&0&0&0&0&0\\&&0&0&0&0\\&&&1&0&0\\&&&&0&0\\&&&&&0\end{bmatrix}+\frac{{}^1\tau_{11}{}^1A}{{}^1L}\begin{bmatrix}1&0&0&-1&0&0\\&1&0&0&-1&0\\&&1&0&0&-1\\&&&1&0&0\\&&&&1&0\\&&&&&1\end{bmatrix} \tag{4}$$

where

$[k]$ = stiffness matrix of a nonlinear equivalent truss element

$[k_e]$ = elastic stiffness matrix

$[k_g]$ = geometric stiffness matrix

${}^1E_{eq}$ = ${}^1E_{\tan}$ or ${}^1E_{\sec}$

${}^1E_{\tan}$ = tangential modulus

${}^1E_{\sec}$ = secant modulus

${}^1\tau_{11}$ = axial stress of a cable member

${}^1A$ = sectional area of a cable member

${}^1L$ = length of a cable members

(Left superscript refers to the occurring configurations as below:
0: initial undeformed configuration, 1: last calculated configuration, 2: current deformed configuration)

$$E_{\tan} = \frac{E}{(1+K_1+K_2)/2\cosh\left(\frac{g_{cb}a}{2T_i}\right)} \tag{5}$$

where

$$K_1 = \frac{1}{g_{cb}a}\left[2T_i \sinh\left(\frac{g_{cb}a}{T_i}\right) - g_{cb}a \cdot \sinh\left(\frac{g_{cb}a}{T_i}\right)\right]$$

$$K_2 = \frac{-4EA}{g_{cb}a}\left[\sinh\left(\frac{g_{cb}a}{2T_i}\right) - \frac{g_{cb}a}{2T_i} \cdot \cosh\left(\frac{g_{cb}a}{2T_i}\right)\right]$$

$$E_{\sec} = \frac{(T_f - T_i)}{\frac{\delta}{c}} = \frac{E}{(1+K_1+K_2)/2\cosh\left(\frac{g_{cb}a}{2T_f}\right)} \tag{6}$$

where

$$K_1 = \frac{1}{g_{cb}a(T_f - T_i)}\left[T_f^2 \sinh\left(\frac{g_{cb}a}{T_f}\right) - T_i^2 \sinh\left(\frac{g_{cb}a}{T_i}\right)\right]$$

$$K_2 = \frac{4EA}{g_{cb}a(T_f - T_i)}\left[T_i \sinh\left(\frac{g_{cb}a}{2T_i}\right) - T_f \sinh\left(\frac{g_{cb}a}{2T_f}\right)\right]$$

g_{cb} = weight per unit length of the cable

T_i = tensile force at condition 1

T_f = tensile force at condition 2

a = horizontally projected length of the cable

To consider the material nonlinearities of steel members modeled by line elements, several methods can be used, such as the plastic zone method, plastic hinge method and refined plastic hinge method. Among these methods, the plastic zone method guarantees the highest numerical accuracy; but it requires much calculation effort and time. So, in this study, the refined plastic hinge method is adopted and used, because of its efficiency and accuracy. The refined plastic hinge method uses the tangential modulus E_t to consider the effect of a gradual yield by axial force, and the scalar parameter η to consider the effect of the gradual yield and plastic hinge occurrence by applied axial force and bending moment (Liew *et al*. 1993, Song and Kim 2007, Kim 2009). The elastic stiffness matrices of the nonlinear frame element and nonlinear equivalent truss element are modified, using the tangential modulus and scalar parameter shown in Eqs. (7)-(10).

$$\begin{aligned} E_t &= E \quad for \;\; P < 0.5P_y \\ E_t &= 4\frac{P}{P_y}\left(1-\frac{P}{P_y}\right) \quad for \;\; P \geq 0.5P_y \end{aligned} \tag{7}$$

where, P=axial force, $P_y = A \cdot F_y$

$$\begin{aligned} \eta &= 1.0 && for \;\; \alpha < 0.5 \\ \eta &= 4\alpha(1-\alpha) && for \;\; \alpha \geq 0.5 \end{aligned} \tag{8}$$

where, α is expresses the level of internal forces of the frame element based on the equation of the beam-column member design in the AISC-LRFD specification (1994), and

$$\alpha = \frac{P}{P_y} + \frac{8M_y}{9M_{yp}} + \frac{8M_z}{9M_{zp}} \qquad for \quad \frac{P}{P_y} \geq \frac{2M_y}{9M_{yp}} + \frac{2M_z}{9M_{zp}}$$

$$\alpha = \frac{P}{2P_y} + \frac{M_y}{M_{yp}} + \frac{M_z}{M_{zp}} \qquad for \quad \frac{P}{P_y} < \frac{2M_y}{9M_{yp}} + \frac{2M_z}{9M_{zp}}$$

where, M_y, M_z=bending moment with respect to the y and z axis of the section, M_{yp}, M_{zp}=plastic moment with respect to the y and z axis of the section

Based on the tangential modulus and scalar parameter η, the elastic stiffness matrix of the nonlinear frame element is rewritten as follows to consider the effect of gradual yield induced by axial force and bending moment:

Bending in the $\hat{x} - \hat{y}$ plane

$$[k] = \frac{EI_z}{L} \times \begin{bmatrix} v_a & \theta_{za} & v_b & \theta_{zb} \\ \frac{3\eta_A + 6\eta_A\eta_B + 3\eta_B}{L^2} & \frac{3\eta_A + 3\eta_A\eta_B}{L} & -\frac{3\eta_A + 6\eta_A\eta_B + 3\eta_B}{L^2} & \frac{3\eta_B + 3\eta_A\eta_B}{L} \\ \frac{3\eta_A + 3\eta_A\eta_B}{L} & 3\eta_A + \eta_A\eta_B & -\frac{3\eta_A + 3\eta_A\eta_B}{L} & 2\eta_A\eta_B \\ -\frac{3\eta_A + 6\eta_A\eta_B + 3\eta_B}{L^2} & -\frac{3\eta_A + 3\eta_A\eta_B}{L} & \frac{3\eta_A + 6\eta_A\eta_B + 3\eta_B}{L^2} & -\frac{3\eta_B + 3\eta_A\eta_B}{L} \\ \frac{3\eta_B + 3\eta_A\eta_B}{L} & 2\eta_A\eta_B & -\frac{3\eta_B + 3\eta_A\eta_B}{L} & 3\eta_B + \eta_A\eta_B \end{bmatrix} \tag{9}$$

Bending in the $\hat{x} - \hat{z}$ plane,

$$\mathrm{k} = \frac{EI_y}{L} \times \begin{bmatrix} w_a & \theta_{ya} & w_b & \theta_{yb} \\ \frac{3\eta_A + 6\eta_A\eta_B + 3\eta_B}{L^2} & -\frac{3\eta_A + 3\eta_A\eta_B}{L} & -\frac{3\eta_A + 6\eta_A\eta_B + 3\eta_B}{L^2} & -\frac{3\eta_B + 3\eta_A\eta_B}{L} \\ -\frac{3\eta_A + 3\eta_A\eta_B}{L} & 3\eta_A + \eta_A\eta_B & \frac{3\eta_A + 3\eta_A\eta_B}{L} & 2\eta_A\eta_B \\ -\frac{3\eta_A + 6\eta_A\eta_B + 3\eta_B}{L^2} & \frac{3\eta_A + 3\eta_A\eta_B}{L} & \frac{3\eta_A + 6\eta_A\eta_B + 3\eta_B}{L^2} & \frac{3\eta_B + 3\eta_A\eta_B}{L} \\ -\frac{3\eta_B + 3\eta_A\eta_B}{L} & 2\eta_A\eta_B & \frac{3\eta_B + 3\eta_A\eta_B}{L} & 3\eta_B + \eta_A\eta_B \end{bmatrix} \tag{10}$$

It should be noted that:

1. When $1 > \eta_A > 0$ and $1 > \eta_B > 0$, these account for the effects of partial yield at both ends of the elements.
2. When $\eta_i = 1$, the section of node i is fully elastic.
3. When $0 < \eta_i < 1$, the section of the node i is partially yielding.

4. When $\eta_i = 0$, the section of node i has fully yielded.

2.1.2 Numerical solution strategy for nonlinear finite element analysis

There are several numerical methods for the numerical strategy of incremental-iterative analysis for nonlinear analysis, such as the Newton-rapshon method, arc-length method, work control method and generalized displacement control method. Because cable-stayed bridges have various geometric and material nonlinearities, complex nonlinear responses may occur when the structure is subjected to external forces. The numerical methods can be classified into several categories, such as the force-control method, displacement-control method, and work control method. In general, a force-control method, such as the Newton-rapshon method, is not appropriate for tracing complex nonlinear response. For the response, a displacement or work control method is widely used. Among these methods, the arc-length method (Crisfield 1983) has been widely used. But, there is a problem in the constrain equation of the method: the units of each term are not the same, and this inequality of units may induce numerical instability, when the structural response reaches towards its ultimate state (Yang and Kuo 1994). So, a generalized displacement control method (Yang and Kuo 1994) is used in this study. Using this method, incremental-iterative load factors are calculated and applied during nonlinear analysis, so that complex nonlinear response of cable-stayed bridges can be traced with numerical stability.

$$\lambda_1 = \pm\lambda_1^1 \left| GSP \right|^{1/2} \qquad (j = 1) \tag{11}$$

$$\lambda_j = -\frac{\left\{\Delta\hat{U}_1^{i-1}\right\}^T \left\{\Delta\bar{U}_j\right\}}{\left\{\Delta\hat{U}_1^{i-1}\right\}^T \left\{\Delta\hat{U}_j\right\}} \qquad (j \geq 2 \tag{12}$$

where

$GSP = \dfrac{\left\{\Delta\hat{U}_1^1\right\}^T \left\{\Delta\hat{U}_1^1\right\}}{\left\{\Delta\hat{U}_1^{i-1}\right\}^T \left\{\Delta\hat{U}_1\right\}}$, Generalized stiffness parameter

λ_j = i-th incremental, j-th iterative analysis load factor

λ_1^1 = preset load increment factor

$\left\{\Delta\bar{U}\right\}$ = incremental displacement vector by unbalanced force vector

$\left\{\Delta\hat{U}\right\}$ = incremental displacement vector by total load vector

(A super script indicates an incremental step while a subscript indicates an iterative step. All quantities with no superscript should be interpreted as those associated with the i-th incremental step.)

The sign of λ_1^1 at the right side in Eq. (11) indicates the load applying direction. If the sign is positive, the incremental load is applied in the same direction as that of the former incremental load. This sign is determined by the sign of *GSP*, the generalized stiffness parameter described in Eq. (12). If *GSP* has a positive sign, the sign of λ_1 has the same sign as that of λ_1^{i-1}, which refers to the former incremental load factor. However, if *GSP* shows a negative sign, the direction of loading is reversed by multiplying the λ_1 by -1.

2.1.3 Nonlinear analysis procedure

Based on the incremental-iterative analysis scheme introduced in previous section, the nonlinear finite element analysis is performed calculating all the displacements and internal forces at every nodes of the analysis model. First of all, the applied external force vector $\{P_j^i\}$ at *j*-th iteration of the *i*-th incremental analysis step can be written as shown in Eq. (13).

$$\{P_j^i\} = \Lambda_j^i \{\hat{P}\} \tag{13}$$

where, $\{\hat{P}\}$ is the reference load vector which denotes the total applied load vector, $\Lambda_j^i = \Lambda_{j-1}^i + \lambda_j^i$ is the load increment parameter at *j*-th iteration of the *i*-th incremental analysis step, λ_j^i =load factor shown in Eqs. (11) and (12)

The incremental-iterative analysis is conducted as follows:

Step 1: Calculate the displacement increments $\{\Delta U_j^i\}$ and load increment parameter λ_j^i

A. For the first iteration (*j*=1) at any incremental step *i*

(a) Set the global structural stiffness matrix $[K_0^i]$

(b) Solve the following equation for calculating the displacement vector $\{\Delta\hat{U}_1^i\}$ due to reference load vector $\{\hat{P}\}$ at the current state

$$[K_{j-1}^i]\{\Delta\hat{U}_1^i\} = \{\hat{P}\} \tag{14}$$

(c) If *i*=1, set GSP as 1.0

If *i*>1, use Eq. (12) to calculate GSP and λ_1^i

(d) If the calculated GSP is negative, multiply the λ_1^i by -1 to reverse the direction of loading

(e) Determine the displacement increments $\{\Delta U_1^i\}$ using Eq. (15)

$$\{\Delta U_j^i\} = \lambda_1^i \{\hat{U}_1^i\} \tag{15}$$

B. For the subsequent iterations (*j*≥2)

(a) Update the global structural stiffness matrix $[K_{j-1}^i]$

(b) Solve the following equations for the displacements $\{\Delta\hat{U}_j^i\}$ and $\{\Delta\bar{U}_j^i\}$ which denote the displacement vector due to reference load vector and unbalanced load vector $\{\hat{R}_{j-1}^i\}$, respectively

$$[K_{j-1}^i]\{\Delta\hat{U}_j^i\} = \{\hat{P}\} \tag{16}$$

$$[K_{j-1}^i]\{\Delta\bar{U}_j^i\} = \{\hat{R}_{j-1}^i\} \tag{17}$$

(c) Determine the load increment parameter λ_j^i by Eq. (12)

(d) Calculate the total displacement increments $\{\Delta U_j^i\}$ for the current iterative step by Eq.

$$\{\Delta U_j^i\} = \lambda_j^i \{\hat{U}_j^i\} + \{\Delta \bar{U}_j^i\} \tag{18}$$

Step 2: Calculate the total applied load vector $\{P_j^i\}$, total structural displacement vector $\{U_j^i\}$, and the load factor Λ_j^i following the equations, respectively.

$$\Lambda_j^i = \Lambda_{j-1}^i + \lambda_j^i \tag{19}$$

$$\{P_j^i\} = \Lambda_j^i \{\hat{P}\} \tag{20}$$

$$\{U_j^i\} = \{U_{j-1}^i\} + \{\Delta U_j^i\} \tag{21}$$

Step 3: Update the shape of the structure considering the displacement increments. For the frame element, update the section axes and element axis.
Step 4: Calculate the internal forces of the every elements
Step 5: Calculate the internal force vector $\{F_j^i\}$ and unbalance force vector $\{R_j^i\} = \{P_j^i\} - \{F_j^i\}$
Step 6: Check the numerical convergence.
Step 7: Re-run Steps 2~6 until the satisfied numerical convergence is obtained.
Step 8: Update i=i+1 and go to Step 1 for next incremental analysis.
Step 9: If the load factor Λ_j^i is reach to the pre-defined total load factor, stop the analysis.

2.2 Algorithm of the cable-failure analysis

Cable failure analysis is performed after the initial shape analysis. As is well known, cable-stayed bridges are designed and constructed with optimal cable tensile forces to obtain the target configuration under a dead load condition. If it is assumed that cable failure occurs after construction, or during use, the cable failure analysis should be performed on the completed model after initial shape analysis, to consider the characteristics of the design and construction of cable-stayed bridges.

To find the new equilibrium state after cable failure, the analysis model that suffers the cable failure is re-built, by removing the failed cable. Also, the internal force vector and external force vector are re-calculated in reference to the rebuilt analysis model. Using these vectors, the unbalanced force vector that should be eliminated is calculated. Then, iterative analysis is performed to eliminate the unbalanced force vector, and find the new-equilibrium position of the structure. After the analysis, the configuration and internal forces of the structure is updated and the structural state after cable failure is obtained.

(1) Perform the initial shape analysis for the completed structure by initial force method (Wang *et al.* 1993)

Step 1: Set the initial shape (or target shape after the initial shape analysis) of the completed structure with considered initial (initial tension of the cables) and external forces at the analysis stage

Repeat step 2~5 until the deformed structural shape converge to the target shape. (*k* of each

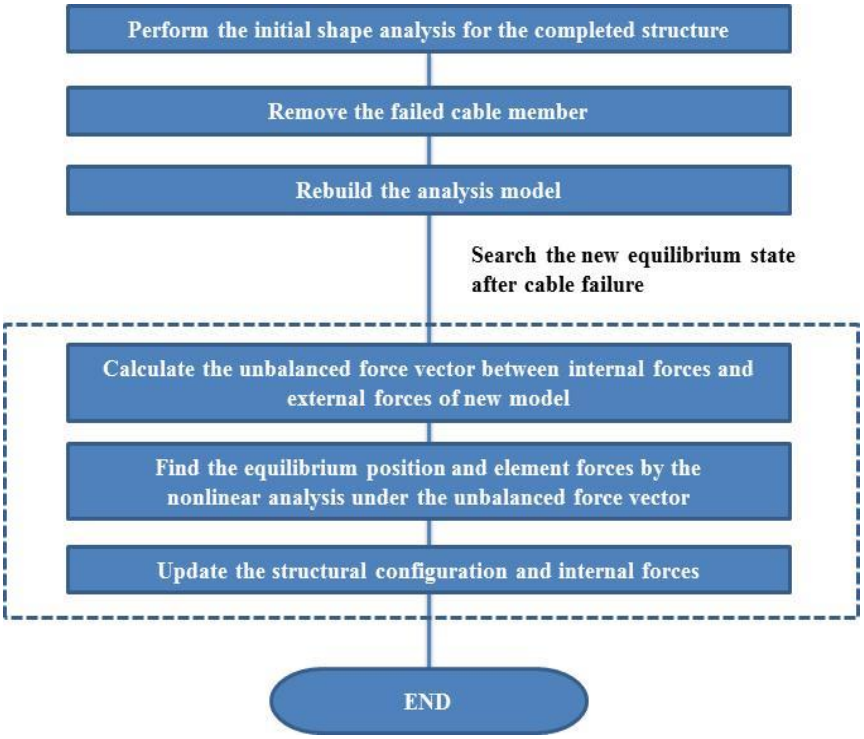

Fig. 3 Procedure of the suggested cable failure analysis

term denotes the iteration number of the initial shape analysis.)

Step 2: Set the external and initial force vectors $\{P^k\}$, $\{IF^k\}=\{F^{k-1}\}$, and global stiffness matrix $[K^{k-1}]$

Step 3: Calculate the displacement increments $\{\Delta U^k\}$ by performing the incremental-iterative analysis

Step 4: Update the position vector $\{L^k\}=\{L^{k-1}\}+\{\Delta U^k\}$ and internal force vector $\{F^k\}$

Step 5: Check the structural deformation

(2) Perform the cable-failure analysis

Step 1: Remove the failed cable members from the whole structural model and set the relevant matrix $\{L_0^m\}$, $\{K_0^m\}$, $\{P_0^m\}$, $\{F_0^m\}$, and unbalance force due to cable element elimination $\{UBF_0\}=\{P_0^m\}-\{F_0^m\}$ (Super script *m* means the cable-failure analysis stage and subscript *j* means the iteration number of the analysis)

Step 2: solve the equation and update the structural states

$$\left[K_{j-1}^m\right]\{\Delta U_j^m\}=\{UBF_j\}$$

$$\{\Delta U_j^m\}=\sum_{n=1}^{j-1}\{\Delta U_n^m\},\quad \{UBF_j\}=\{P_0^m\}-\{F_j^m\}$$

Repeat step 2 until the unbalanced force vector vanish.

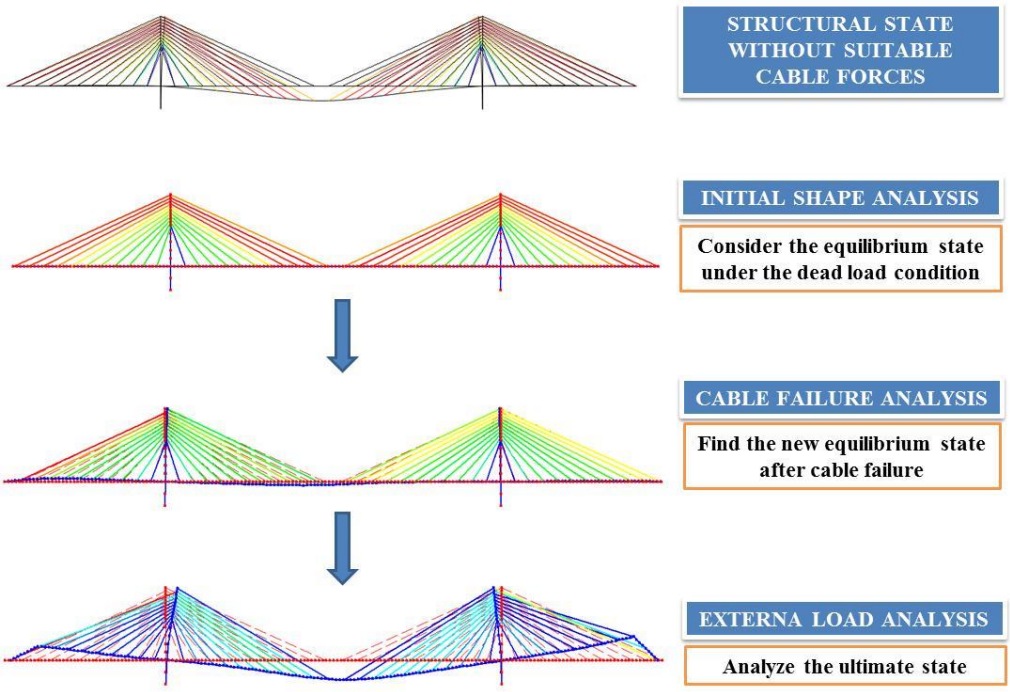

Fig. 4 Proposed analysis strategy of ultimate analysis for steel cable-stayed bridges after cable failure

2.3 Analysis strategy of ultimate analysis for steel cable-stayed bridges after cable failure

The ultimate behavior of steel cable-stayed bridges after cable failure is analyzed by a three-step analysis scheme, as shown in Fig. 4. Firstly, initial shape analysis is performed to determine optimal tensile forces of the stay cables, which ensure that the structure suffers minimal deformation under the dead load condition, and to consider the structural state before cable failure analysis. Secondly, cable failure analysis is performed to find the new equilibrium state after cable failure. Finally, external load analysis is performed to trace the nonlinear response, and to find the ultimate behavior under specific external load condition.

All three analyses, initial shape analysis, cable failure analysis and external load analysis, are performed based on the theory of nonlinear finite element analysis; thus geometric and material nonlinearities of steel cable-stayed bridges are considered during the analyses. The analysis program was written using Visual C++ V6.0. As well as the numerical modulus, a simple post processor is also made, to intuitively observe the structural behavior.

Validations of the consideration method for the geometric and material nonlinearities, including the initial shape analysis method, were performed in former papers and researches (Yang and Kuo 1994, Song *et al* 2006, Lim *et al* 2008, Song and Kim 2007, Kim 2009, Kim *et al*. 2015). Also, the cable failure analysis is basically based on the construction stage analysis of cable stayed bridges, via backward process analysis. So, detailed description of the validations of the nonlinear analysis algorithms is omitted in this paper. Also the validation of the cable failure analysis is replaced by the qualitative estimation of the following case studies.

3. Change of statical behavior and ultimate capacity after cable failure

In this chapter, the change of structural state and ultimate behavior after cable failure are studied and described. Firstly, failure cases of a single cable are considered in this study. Using the proposed analysis method, the changes of configuration, bending moment diagram of the girder, and tensile force distribution of stay cables after the cable failure are analyzed. Also, the changes of ultimate behavior and load carrying capacity under specific live load conditions are studied, by considering each cable failure case.

3.1 Analysis model

Fig. 5 shows the analysis models considered in this study. The model is a 900.0 m long (220.0+460.0+220.0), fan type, steel cable-stayed bridge. Fig. 6 shows a section of the girder. The section of the girder is designed as a four cell steel box. The section of the mast is considered as a box section. It is assumed that there are sufficient stiffeners to prevent local buckling in the sections of the girder and mast. Table 1 represents the material and geometric properties of girder, mast, and cables. The girder and mast are modeled by a nonlinear frame element, while the cable is modeled by a nonlinear equivalent truss element, as introduced in the previous chapter.

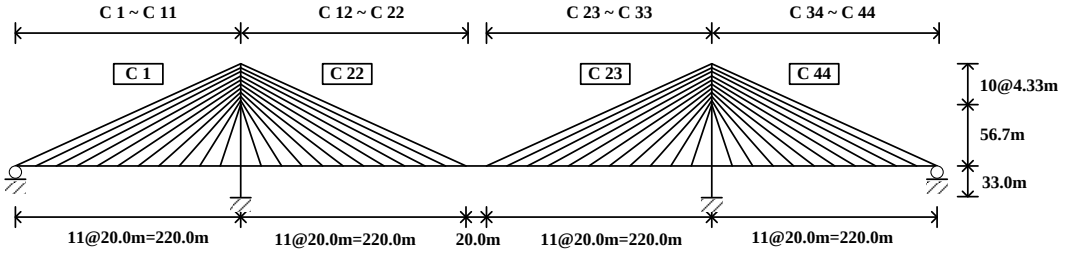

Fig. 5 Completed analysis model

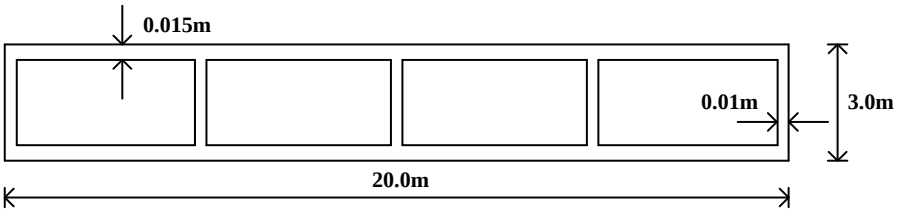

Fig. 6 Section of the girder

Table 1 Material and geometric properties of the main members

	Girder	Mast	Cable
Elastic modulus (E, kN/m^2)	2.1×10^8	2.1×10^8	2.1×10^8
Sectional area (A, m^2)	0.750	0.792	0.021
2nd moment of inertia (I, m^4)	1.446	3.143	-
Weight per unit volume (γ, kN/m^3)	218.27	78.0	78.0
Yield stress (Fy, MPa)	380.0	Elastic	1,800.0

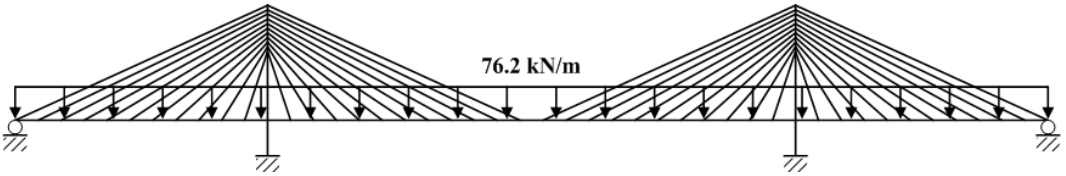

(a) Live load case 1

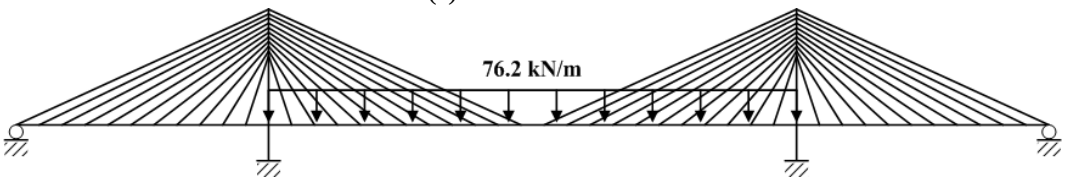

(b) Live load case 2

Fig. 7 Considered live load cases

Fig. 7 presents the considered live load cases after cable failure. Live load cases that are acting vertically distributed on the girder are designed by reference to the Korean Highway Bridges Design Code (Ministry of Land, Infrastructure and Transport 2010). The live loads assumed by traffic load are 12.7 kN/m/lane, and a six-lane road condition is assumed for each bridge.

3.2 Change of structural state after cable failure

It can be simply supposed that if the cable is broken or fails, the forces that had been supported by the cable are transferred to other cables nearby the broken cable. Under this behavior, the region that had been supported by the broken cable suffers local deflection, and the tensile forces of the cables nearby the broken cable increase.

In this chapter, the structural change after cable failure is described in reference to the analysis results, using the analysis method suggested in this study. As mentioned previously, failure cases of a single cable are assumed, thus a total 22 cases of cable failure are considered in this study (cable 1~cable 22). For qualitative and quantitative study, change of the important internal force distribution with deformed shapes is described in detail.

3.2.1 Structural behavior after the failure of side-span cables (cable 1~cable 11 in left side span)

As shown in Fig. 8, a local deflection at the region supported by the broken cable occurs when the cable fails, except for cable 1, the exterior cable of the left side span. When cable 1 breaks, there is lifting of the side span, although the cable, one of the supports of the side span, is broken. This interesting behavior is induced by the following sequence. When the cable is broken, additional horizontal force acts on the top of the mast, which causes horizontal movement of the mast to the center. As the mast horizontally moves to the center, the side span is lifted, because of the stay cables of the side span. This behavior occurs when the exterior cable is broken. The reason is as follows: A. The exterior cable has the largest tensile force and lowest horizontal stay angle, so the largest additional horizontal force is caused when the cable is broken. B. The cable had hung on the top of the mast, so larger additional force causes larger flexural deformation of the mast.

Moreover, there is another difference. When the exterior cable of the left side span is broken, the center span and right side span also suffer significant deformation, while there is no significant

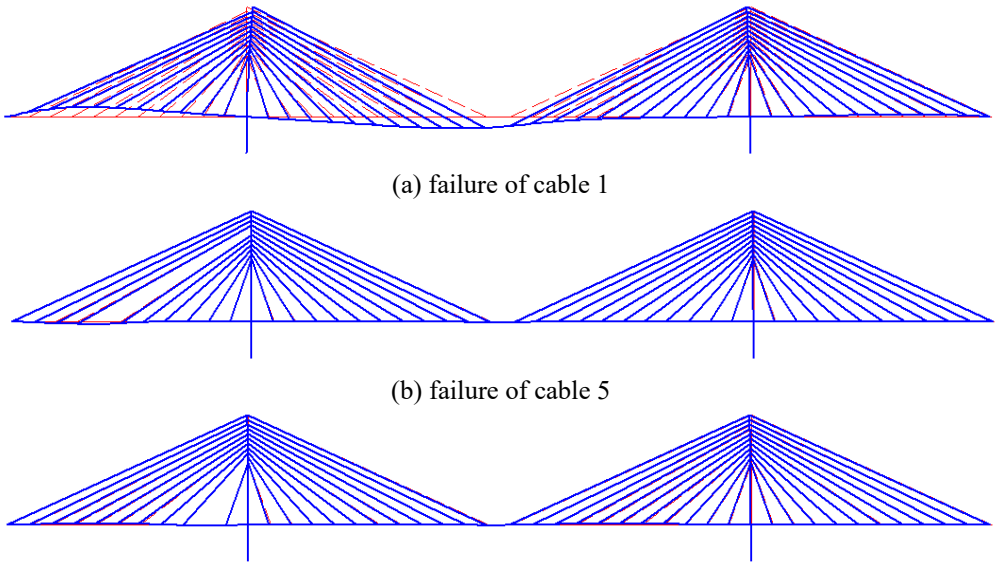

(a) failure of cable 1

(b) failure of cable 5

(c) failure of cable 10

Fig. 8 Deformed shape after the failure of side-span cables (scale factor : 20.0)

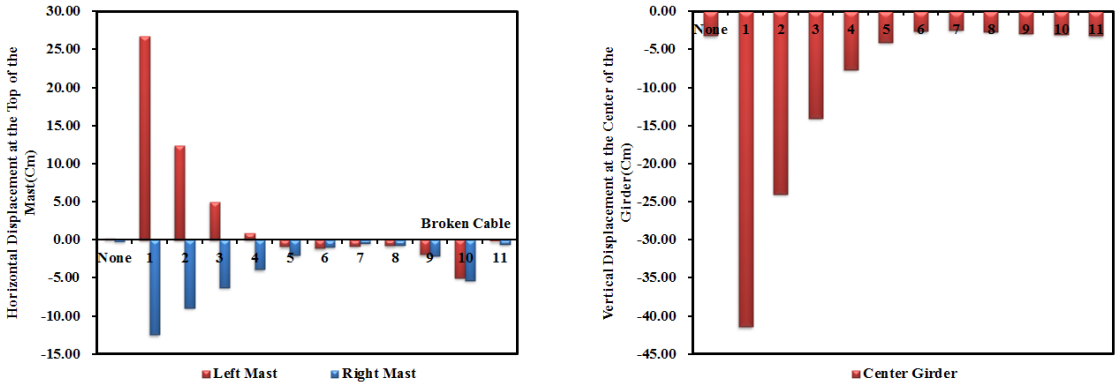

(a) horizontal displacement of the top of the mast (b) vertical deflection of the center of the center span

Fig. 9 Displacement of the masts and girder after the failure of side-span cables

("None" means the undamaged structure.)

deformation when the interior cables of the left side span are broken. This can be also explained by the same reason previously mentioned. As the left mast suffers horizontal movement after the exterior cable is broken, the center span suffers downward deflection, and the deflection of the center span induces the horizontal movement of the right mast to the center. Also, horizontal movement of the right mast causes lift of the right side span. But, similar interactive behavior rarely occurs when interior cables in the left side span are broken. When these cables are broken, significantly only local deflection occurs. This difference of behavior after cable failure is quite relative to the initial tensile force, stay angle and hanging location of the broken cable. In summary, it can be said that global change of the structural configuration is induced by the

breaking of a stay cable that has large initial tensile force, low horizontal stay angle, and high hanging location. But in general the cable which is highly hung has a lower horizontal angle, and thus has higher initial tensile force. So, it can be supposed that the failure of exterior cables in the side or center span may make for global structural change. This tendency is well shown also in Fig. 9.

Fig. 10 presents the change of tensile forces of stay cables after a cable's failure. When a cable breaks, the load that had been supported by the broken cable is transferred to other cables nearby the broken cable. So, the cables nearby the broken cable show an increase of tensile force. This is a simple situation. In addition, if a global change of structural configuration occurs, other cables far from the broken cable may suffer significant change of tensile force. As shown in Fig. 10, cables of other spans, as well as the left side span, show change of their tensile forces when an exterior cable is broken. But, few cables nearby the broken cable show force change when an interior cable is broken. It means that the failure of a stay cable that had large tensile force and was highly hung, leads to global change of the structure.

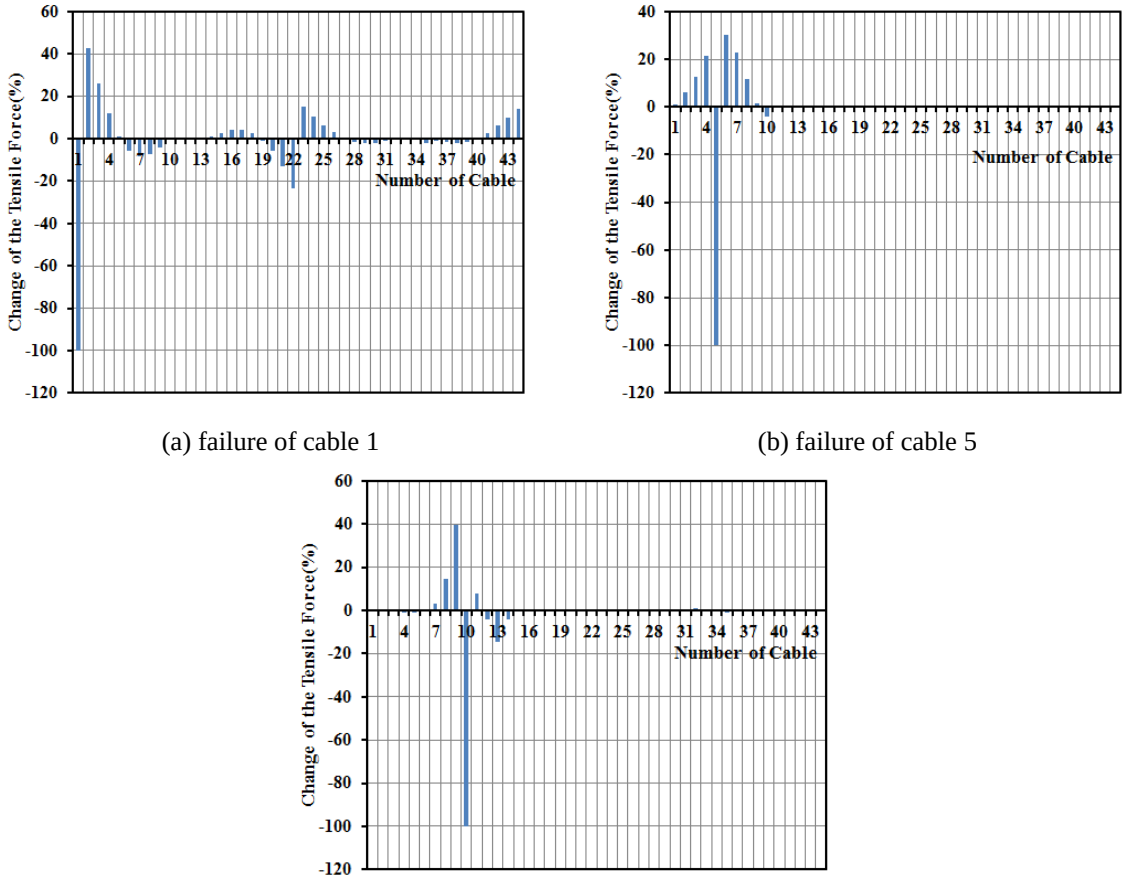

(a) failure of cable 1

(b) failure of cable 5

(c) failure of cable 10

Fig. 10 Change of the tensile forces of stay cables after the failure of side-span cables (Change of tensile forces (%)=(changed force–initial force)/initial force×100(%))

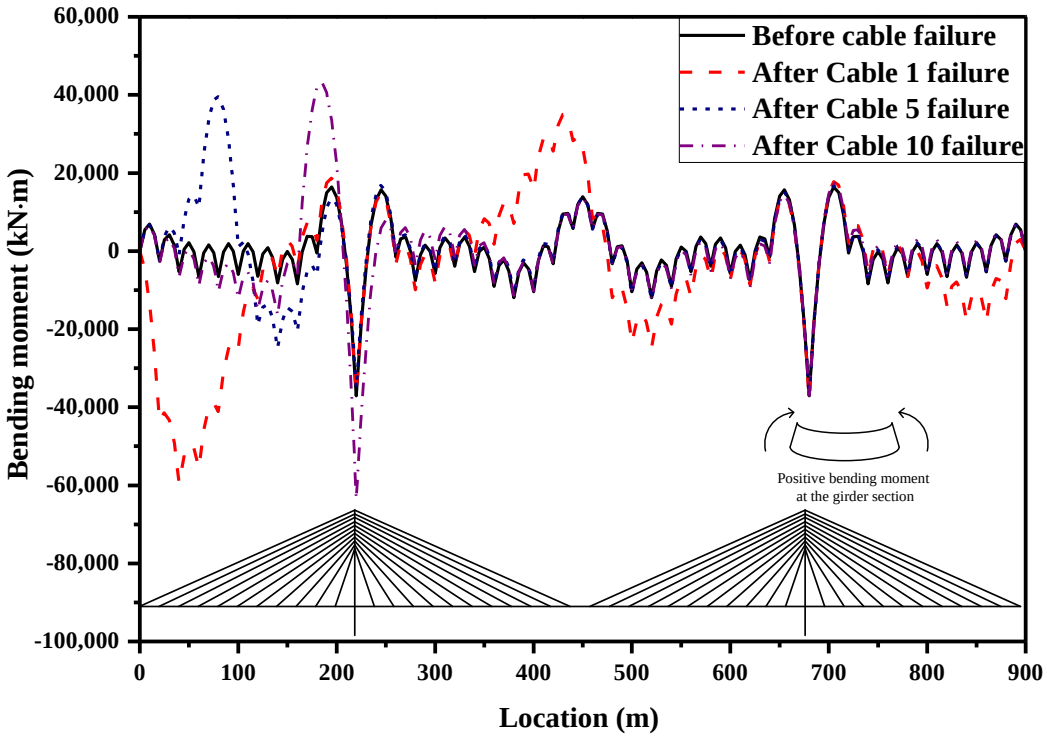

Fig. 11 Change of the bending moment distribution of the girder after the failure of side-span cables

Fig. 11 shows the change of bending moment diagram of the girder, after the failure of a cable of the left side span. First, when cable 5 or 10, one of the interior cables of the left side span, is broken, there is local increase of the bending moment at the section that had been supported by the broken cables. After the failure of these cables, each section that had been supported by those cables shows 140.7% and 71.4% of positive bending moment increase, respectively. Also, a significant increase of negative bending moment at the joint between the girder and left mast occurs when cable 10, nearby the left mast, fails. But, those significant bending moment changes occur at the left side span when those cables are broken.

In contrast, global change of the bending moment distribution of the girder occurs when cable 1, the exterior cable of left-side span, is broken. It is basically induced by a global change of the structural configuration, as previously described. Because of the global structural behavior after a cable failure, every span definitely suffers a change of bending moment distribution, and a significant increase of positive and negative bending moment occurs. After cable failure, negative bending moment is widely distributed at the left side span, because of the upward deformation of the left side span. Also, positive bending moment nearby the center of the center span largely increases, because of the downward deflection. Because of the failure of a cable, 60.0% and 113.3% of increase of the maximum positive and negative bending moment occurs.

In summary, if a cable that has large tensile force, low stay angle and is hung on a high position breaks, global structural change occurs. Also, this leads to significant change of the internal force distribution, and increase of the maximum/minimum internal force.

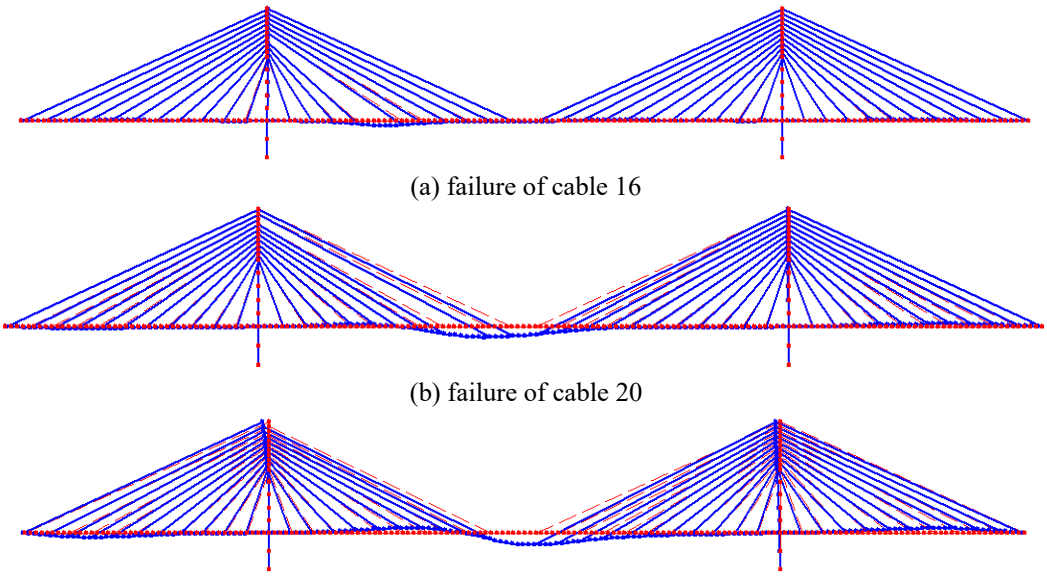

(a) failure of cable 16

(b) failure of cable 20

(c) failure of cable 22

Fig. 12 Deformed shape after the failure of center-span cables (scale factor: 20.0)

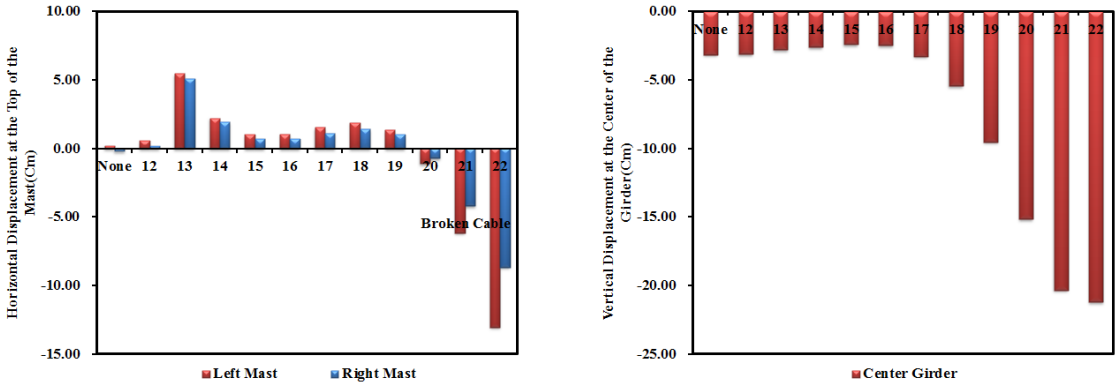

(a) horizontal displacement of the top of the mast (b) vertical deflection of the center of the center span

Fig. 13 Displacement of the masts and girder after the failure of center-span cables

3.2.2 Structural behavior after the failure of center-span cables (cable 12~cable 22 in the center span)

Fig. 12 shows the deformed shapes after the failure of center-span cables.

In this case of cable failure at the center span, a similar structural behavior occurs to the case of failure at the left side span. When interior cables of the center span break, local deformation mainly occurs; while global structural change occurs when the exterior cable which is nearby the center breaks. Because cable 22, the exterior cable of the center span, had the largest initial tensile force and was hung on top of the mast among the center cables, a large horizontal movement of the left mast occurs when the cable fails. After the left mast moves horizontally, the left part of the center span suffers uplift by the movement of the left mast, and the left side span vertically

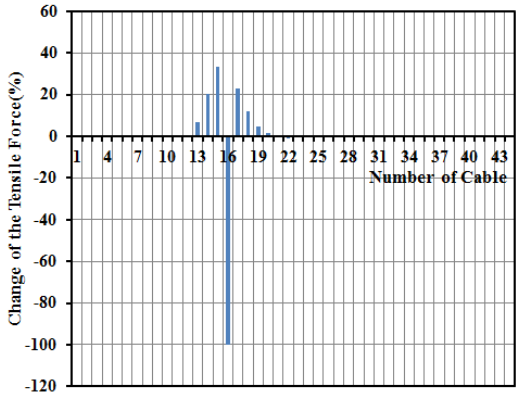

(a) failure of cable 16

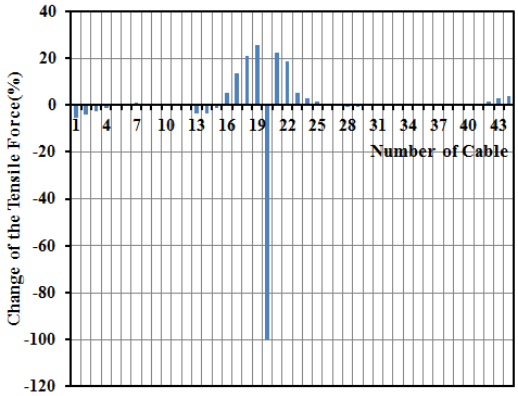

(b) failure of cable 20

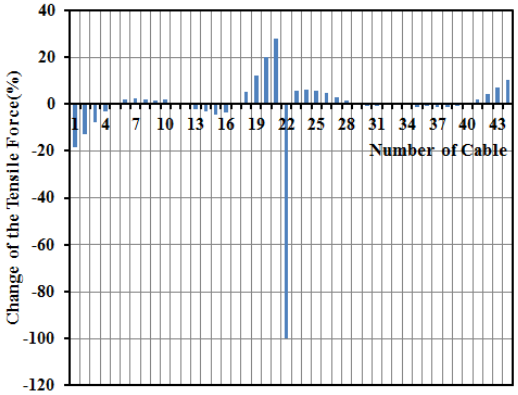

(c) failure of cable 22

Fig. 14 Change of the tensile forces of stay cables after the failure of center-span cables

deflects. Also, the right part of the center span suffers downward deflection, the deflection leads to the horizontal movement of the right mast, and finally the right span is uplifted. The sequence and reason of global behavior after a center cable fails is almost the same as the behavior after a side span cable fails. So, similar change of the internal forces can also be supposed. Fig. 13 indicates that the failure of a cable that was nearby the center and had a large initial tensile force with a low stay angle, generally leads to large deformation.

As shown in Fig. 14, the failure of the cable nearby the center of the center span leads to the change of forces of other cables in both side spans, as well as in the center span. Fig. 15 also indicated that if a cable fails that had large initial tensile force, low stay angle and was highly hung, global change of the bending moment distribution of the girder occurs, because of a significant global change of the structural configuration. Similar to the situation of cable failure at the side span, a large increase of positive and negative bending moment occurs, as well as significant change of the bending moment distribution, although only one cable fails. This is due to the structural characteristics of cable-stayed bridges. The structure consists of the girder, mast and stay cables. The cable, the intermediate support of the girder, tightly connects the girder with mast. Because of the geometric characteristics, interaction between girder, mast and cables definitely

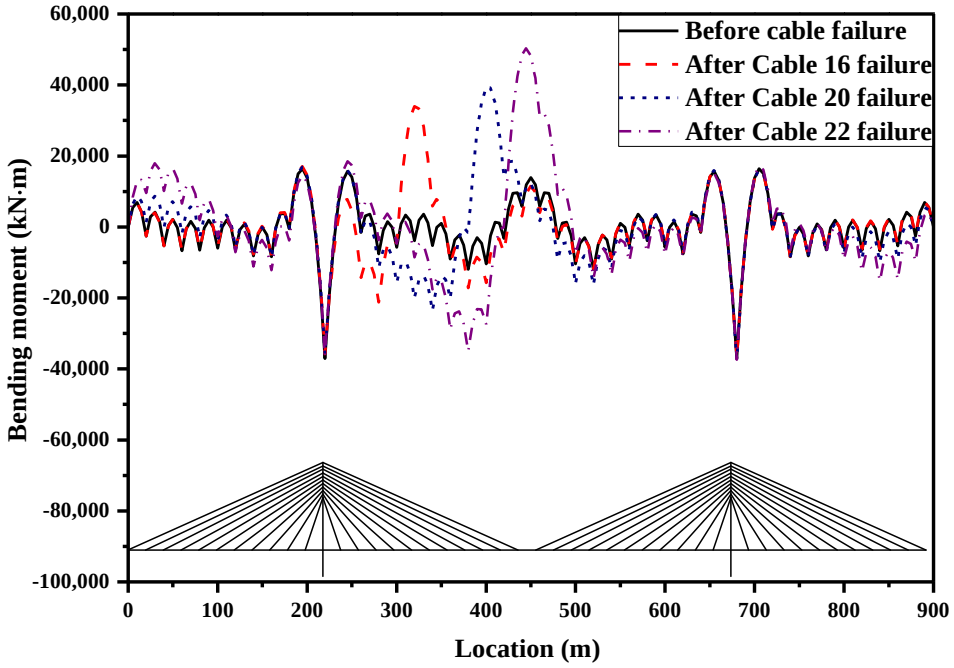

Fig. 15 Change of the bending moment distribution of the girder after the failure of center-span cables

occurs. Also, the structural state and equilibrium condition may be heavily affected by local structural change, because of the interaction. Moreover, the structure is designed and construction based on an optimum structural state, based on construction stage analysis and initial shape analysis. So, the structure is quite sensitive to cable failure, although only a few cables are broken or fail.

3.3 Change of the ultimate behavior after the cable failure

In this chapter, the change of the ultimate behavior after cable failure is described. To compare the ultimate behavior before and after cable failure, the behavior of a healthy structure under the considered live load condition shown in Fig. 7 is introduced first. After that, the ultimate behavior after cable failure, obtained by the proposed ultimate analysis sequence, is compared with the ultimate behavior before cable failure.

3.3.1 Ultimate behavior before cable failure

Fig. 16 shows the load-displacement curves at the center of the center span, under the specific live load cases shown in Fig. 5.

Under LC1 (Live load case 1), the first plastic hinge occurs at the sections nearby the joint between the girder and both masts, due to excessive negative bending moment and compressive force. As the live load increases, the yield region is enlarged to other sections nearby the joint. In addition, the exterior cables of both the side span and center span yield, as the live load continuously increases. Finally, the live load factor starts to decrease when a plastic hinge occurs at the center of the center span, and the structure reaches the ultimate state.

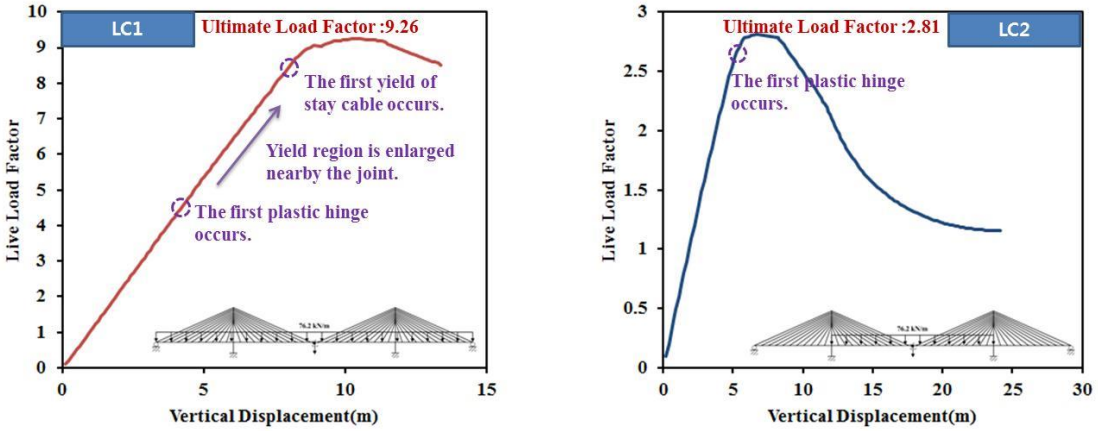

(a) Load case 1 (LC1) (b) LC2

Fig. 16 Load-displacement curve at the center of the center span

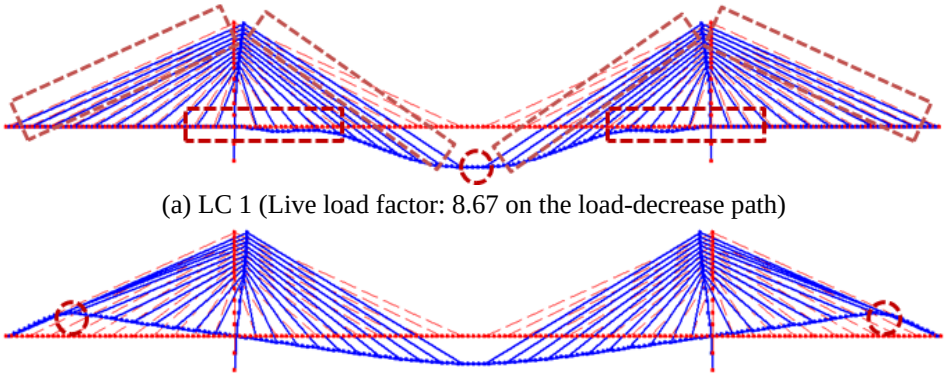

(a) LC 1 (Live load factor: 8.67 on the load-decrease path)

(b) LC 2 (Live load factor: 2.68 on the load-decrease path)

Fig. 17 Ultimate mode shape (Scale factor: 3.0, Red line: the region or member that yields.)

Under LC2, vertically distributed force at the center span, both masts first suffer horizontal movement to the center, because of the deflection of the center span. The horizontal movement causes uplift of the side spans. As the external force increases, negative flexural deformation of the side span is amplified by the beam-column effect induced by the initial uplifting and increasing compressive force. Finally, plastic hinges occur at the sections nearby the ends of both side spans, due to excessive negative bending moment and compressive force, and the structure reaches the ultimate state. According to the analysis result, the ultimate load factor under LC2 is quite a bit lower than the value under LC1, although the external force is acting on only the center span.

3.3.2 Ultimate behavior after cable failure

Fig. 18 shows the load-displacement curve at the center of the center span when cable 1 breaks. Comparing with the curves of the non-cable broken model, there is significant difference under LC1. After the first plastic hinge occurs, the live load factor starts to decrease, while the structure that doesn't suffer cable failure shows several material yields before the ultimate state. Also, the

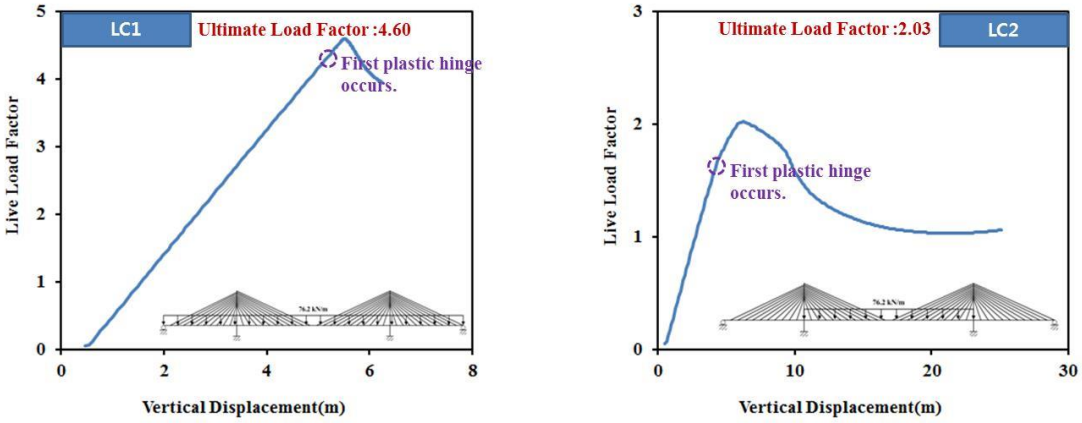

(a) LC1 (b) LC2

Fig. 18 Load-displacement curve at the center of the center span after the failure of cable 1

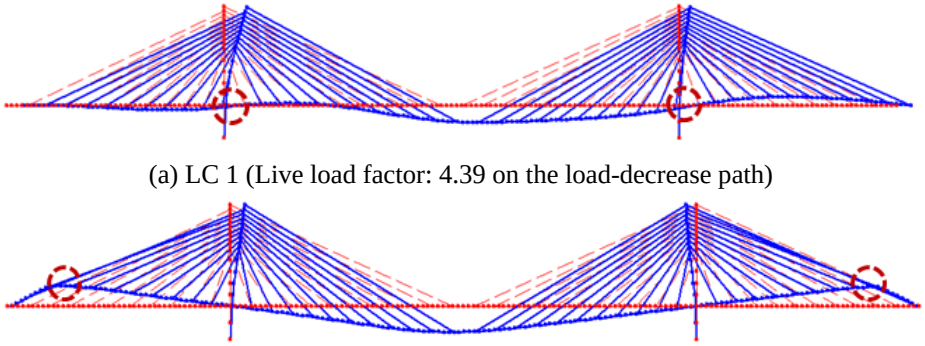

(a) LC 1 (Live load factor: 4.39 on the load-decrease path)

(b) LC 2 (Live load factor: 1.87 on the load-decrease path)

Fig. 19 Ultimate mode shape after the failure of cable 1 (Scale factor: 3.0, Red line: the region or member that yields)

ultimate load factor under LC1 heavily decreases, compared with the result of the non-cable broken model. Although the general pattern of ultimate behavior of the cable broken structure does not significantly change under LC2, the result shows 27.8% decrease due to loss of stiffness and asymmetric behavior after the cable failure.

There is a big difference of deformed shapes under LC 1, while the deformed shapes of the cable failed model are similar to those of the non-failed model under LC2. Under LC1, asymmetric horizontal movement of the structure obviously occurs, although symmetric external load is applied to the girder. This structural behavior is consequently induced by the asymmetry of the structure after the cable failure. When symmetric external force is vertically applied to the girder of symmetric cable-stayed bridges, horizontal forces are applied to both masts, because of the difference of the lengths between the side span and center span. These two horizontal forces applied to both masts show the same absolute value, but different direction. So, the forces cancel one another. But when the cable breaks, the absolute values of horizontal forces applied to both masts may be different. Actually, although the cable is broken, the resultant of the required vertical

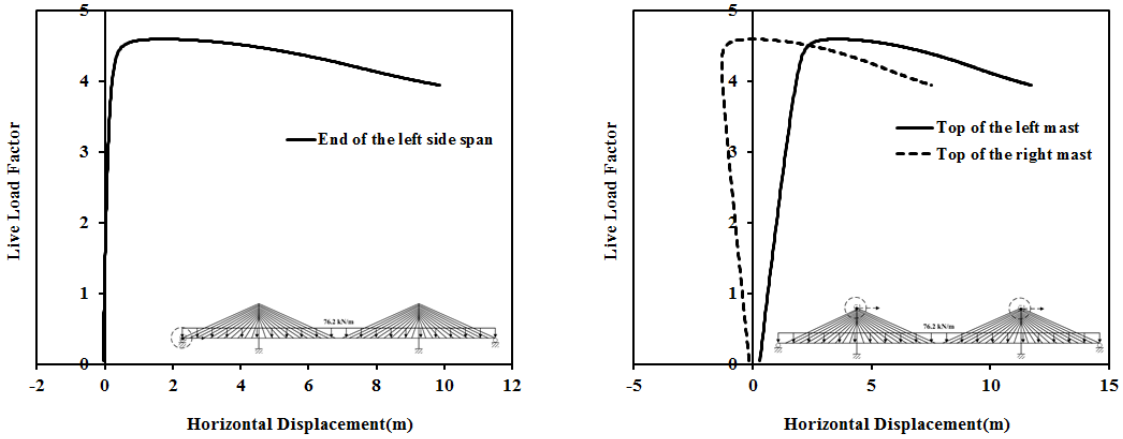

(a) End of the left side span (b) Tops of both masts

Fig. 20 Load-displacement curves for horizontal movement under LC1 when cable 1 breaks

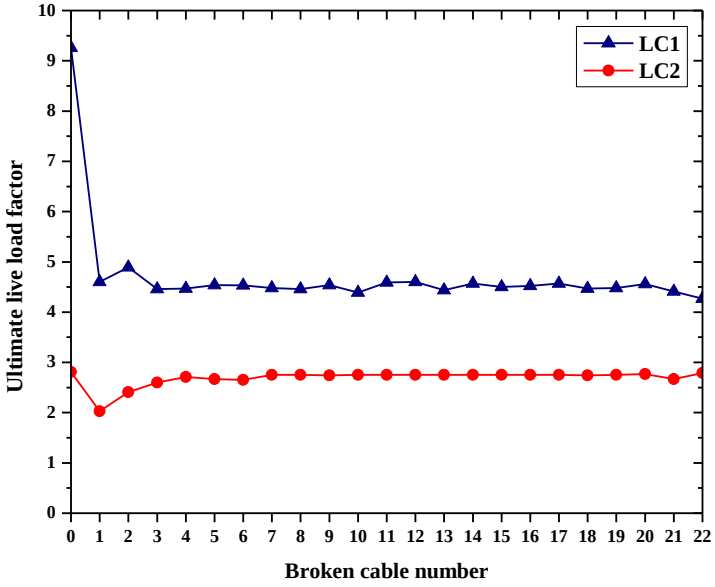

Fig. 21 Change of the ultimate load carrying capacity after cable failure (*0 of the *x* axis means "intact condition")

forces to resist vertical external forces is almost the same if the same vertical external force is applied. But, the distribution of tensile force to make the required vertical forces becomes different, because of the structural asymmetry caused by the cable failure. Also, the asymmetric distribution of the tensile force of stay cables induces magnitude inequality of the horizontal force acting on the top of both masts. So, the structure suffers horizontal movement, as well as deformation by the beam-column effect of the girder and mast. Fig. 20 clearly shows the amplified horizontal movement, via load-displacement curves for the horizontal displacements of the girder and masts.

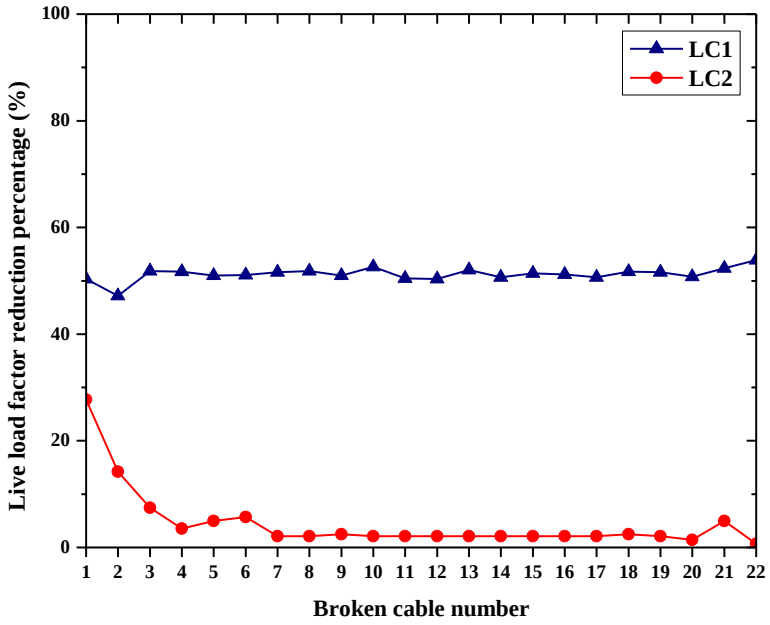

Fig. 22 Reduction percentage of the ultimate load carrying capacity after cable failure

As shown in Fig. 20, amplification of the horizontal displacement of the girder and both masts occurs, although the external load decreases. In particular, change of the direction of horizontal movement occurs at the right mast. This is definitely due to the asymmetry of the structure by cable failure. Also, it can be said that the amplified horizontal movement is the governing factor for the ultimate behavior under LC1.

The asymmetric behavior also occurs under LC2. But in this case, a critical plastic hinge occurs before horizontal movement is amplified by the structural asymmetry.

Figs. 21 and 22 show the change of ultimate load carrying capacity after cable failure. According to the result, there is a 47.2~53.9% decrease of load carrying capacity under LC1, while a 0.7~27.8% decrease occurs under LC2, although only one cable fails. When cable 1, the exterior cable of left side span, fails, a relatively large decrease of load carrying capacity occurs under LC1. This is due to the uplifting deformation induced by the failure of cable 1, as described before. After the exterior cable of the left side span breaks, the side span suffers upward flexural deformation because of the horizontal movement of the left mast, and the negative bending moment rapidly and substantially increases. Because the governing factor for the ultimate behavior under LC2 is material yield by excessive negative bending moment and compressive force at the section nearby the ends of both side spans, the load carrying capacity also decreases rapidly, although other cable failure cases rarely show significant decrease of the load carrying capacity under LC2. In contrast, every considered case of cable failure shows significant decrease of the load carrying capacity under LC1. This is due to asymmetric structural behavior after cable failure. After cable failure, the ultimate behavior changes. In the asymmetric structural behavior under LC1, the structure mainly becomes the ultimate state by large horizontal displacement, with flexural deformation of the girder and mast. Cable failure may change the ultimate behavior, and rapidly drop the ultimate load carrying capacity down, although only a single cable has failed.

4. Conclusions

In this study, the change of structural state and ultimate behavior after cable failure was investigated. For the study, a cable failure analysis method and a procedure for ultimate analysis of cable-stayed bridges suffering cable failure is suggested and used.

According to this study, cable failure may cause significant change of the structural state, including change of structural configuration and distribution of essential internal forces, such as cable tensile forces and bending moment of the girder. Also, a large increase of the bending moment of the girder is induced via cable failure. When a cable that had large tensile force, low stay angle, and that had been hung on a high position fails, a global configuration change is induced, and leads to global change of the structural state.

Cable failure also leads to significant change of ultimate behavior and load carrying capacity under specific live load conditions. The significant change is basically induced by the asymmetry of the structure caused by the cable failure. According to this study, cable failure may cause heavy decrease of load-carrying capacity, although only a single cable fails.

In this study, individual cable failure is considered as a failure event for a two-dimensional structure. For more intensive investigation of the structural behavior after cable failure, a study considering more various cases of cable failure is needed, including three-dimensional behavior of the structure.

References

Adeli, H. and Zhang, J. (1994), "Fully nonlinear analysis of composite girder cable-stayed bridges", C*omput. Struct.*, **54**(2), 267-277.

Chen, D.W., Au, F.T.K., Tham, L.G. and Lee, P.K.K. (2000), "Determination of initial cable forces in prestressed concrete cable-stayed bridges for given design deck profiles using the force equilibrium method", C*omput. Struct.*, **74**, 1-9.

Cheng, J. and Xiao, R.C. (2004), "Probabilistic determination of initial cable forces of cable-stayed bridges under dead loads", *Struct. Eng. Mech.*, **17**(2), 267-279.

Crisfield, M.A. (1983), "An arc-length method including line searches and accelerations", *Int. J. Numer. Meth. Eng.*, **19**, 1269-1289.

Ernst, H.J. (1965), "Der e-modul von seilen unter berucksichtigung des durchanges", *Der Bauingenieur*, **40**, 52-55. (in German)

Fleming, J.F. (1979), "Nonlinear static analysis of cable-stayed bridges", C*omput. Struct.*, **10**, 621-635.

Freire, A.M.S., Negrao, J.H.O. and Lopes, A.V. (2006), "Geometric nonlinearities on the static analysis of highly flexible steel cable-stayed bridges", C*omput. Struct.*, **84**, 2128-2140.

Gimsing, N.J. (1983), *Cable supported bridges Concept & Design*, 2nd Edition, John Wiley & Sons Ltd., New York.

Kim, K.S. and Lee, H.S. (2001), "Analysis of target configurations under dead loads for cable-supported bridges", C*omput. Struct.*, **79**, 2681-2692.

Kim, S. (2010), "Ultimate Analysis of Steel Cable-stayed Bridges", Ph.D. Dissertation, Korea University, Seoul, Korea.

Lim, N.H., Han, S.Y., Han, T.H. and Kang, Y.J. (2008), "Parametric study on stability of continuous welded rail track - ballast resistance and track irregularity", *Int. J. Steel. Struct.*, **8**(3), 171-81.

Ministry of Land, Infrastructure and Transport (2010), *Korean Highway Bridge Design Code*, Seoul, Korea.

Raftoyiannis, I.G., Konstantakopoulos, T.G. and Michaltsos, G.T. (2014), "Dynamic response of cable-stayed bridges subjected to sudden failure of stays-the 2D problem", *Coupled Syst. Mech.*, **3**(4), 345-365.

Reddy, P., Ghaboussi, J. and Hawkins, N.M. (1999), "Simulation of construction of cable-stayed bridges", *J. Bridge. Eng.*, **4**(4), 249-257.
Ren, W.X. (1999), "Ultimate behavior of long-span cable-stayed bridges", *J. Bridge. Eng.*, **4**(1), 30-36.
Shu, H.S. and Wang, Y.C. (2001), "Stability analysis of box-girder cable-stayed bridges", *J. Bridge. Eng.*, **6**(1), 63-68.
Song, M.K., Kim, S.H. and Choi, C.K. (2006), "Enhanced finite element modeling for geometric non-linear analysis of cable-supported structures", *Struct. Eng. Mech.*, **22**(5), 575-597.
Song, W.K. and Kim, S.E. (2007), "Analysis of the overall collapse mechanism of cable-stayed bridges with different cable layouts", *Eng. Struct.*, **29**, 2133-2142.
Tang, C.C., Shu, H.S. and Wang, Y.C. (2001), "Stability analysis of steel cable-stayed bridge", *Struct. Eng. Mech.*, **11**(1), 35-48.
Wang, P.H. and Yang, C.G. (1993), "Parametric studies on cable stayed bridges", *Comput. Struct.*, **60**(2), 243-260.
Wang, P.H., Lin, H.T. and Tang, T.Y. (2002), "Study on nonlinear analysis of a highly redundant cable-stayed bridges", *Comput. Struct.*, **80**, 165-182.
Wang, P.H., Tang, T.Y. and Zheng, H.N. (2004), "Analysis of cable-stayed bridges during construction by Cantilever methods", *Comput. Struct.*, **82**, 329-346.
Wang, P.H., Tseng, T.C. and Yang, C.G. (1993), "Initial shape of cable stayed bridge", *Comput. Struct.*, **47**(1), 111-123.
Xi, Y. and Kuang, J.S. (1999), "Ultimate load capacity of cable-stayed bridges", *J. Bridge. Eng.*, ASCE, **4**(10), 14-22.
Yang, Y.B. and Kuo, S.R. (1994), *Theory and Analysis of Nonlinear Framed Structures*, Prentice-Hall, Inc., Singapore.

CC